Vol. 605: 73–86, 2018
https://doi.org/10.3354/meps12739

MARINE ECOLOGY PROGRESS SERIES
Mar Ecol Prog Ser

Published October 26

Effects of *Ulva prolifera* blooms on the carbonate system in the coastal waters of Qingdao

Xue Deng[1], Tao Liu[2], Chun-Ying Liu[1,3,*], Sheng-Kang Liang[3], Yu-Bin Hu[4], Yue-Mei Jin[2], Xu-Chen Wang[1,3]

[1]College of Chemistry and Chemical Engineering, Ocean University of China, Qingdao 266100, PR China
[2]College of Marine Life Sciences, Ocean University of China, Qingdao 266100, PR China
[3]Key Laboratory of Marine Chemistry Theory and Technology, Ministry of Education, Qingdao 266100, PR China
[4]Institute of Marine Science and technology, Shandong University, Qingdao 266237, PR China

ABSTRACT: This study investigated the effects of a bloom of the macroalga *Ulva prolifera* on the carbonate system in the Yellow Sea. Two cruises were carried out in the coastal waters of Qingdao, one during *U. prolifera* late bloom stages in 2015 and one after the bloom. In parallel, an 8 d incubation experiment was conducted to determine the variation in the seawater carbonate system during the late bloom period. During the late bloom period, pH was decreased by 0.06 units, while the concentrations of dissolved inorganic carbon (DIC), total alkalinity (TA) and the values of partial pressure of CO_2 (pCO_2) were increased by 27 µmol kg^{-1}, 57 µmol kg^{-1} and 77 µatm in surface waters compared with those after the bloom, respectively. The mean (±SD) air–water CO_2 flux during the first cruise was estimated to be 0.82 ± 0.88 mmol m^{-2} d^{-1}, while it declined to −1.31 ± 2.41 mmol m^{-2} d^{-1} during the second cruise. During both cruises, the pH decreased with depth, and this trend was reversed for DIC, whereas small variations in TA were detected throughout the water column. Comparing final data of the incubation experiment with initial values showed that pH was reduced by 0.23 ± 0.01 units, while DIC and TA increased on average by 71 ± 37 and 37 ± 18 µmol kg^{-1}, respectively. The release of CO_2 from *U. prolifera* occurred rapidly during the late bloom period, which resulted in conversion of Qingdao coastal waters from a sink to a weak CO_2 source.

KEY WORDS: *Ulva prolifera* · Carbonate system · Southern Yellow Sea · Late bloom period

INTRODUCTION

Ulva prolifera is the main causative species of coastal green macroalgal blooms that result from the accumulation of free-floating macroalgae. This phenomenon has been a persistent feature in eutrophic coastal waters and estuaries worldwide (Lin et al. 2011, Guidone & Thornber 2013). Qingdao, a major city on the west coast of the Yellow Sea, has experienced a *U. prolifera* bloom every summer since 2007. The bloom not only substantially alters marine community structure and function, but also produces noxious odors and noxious-smelling deposits on beaches, causing economic losses for the tourism industry and environmental problems for local citizens and governments (Ye et al. 2011, Hu et al. 2015, Y. Li et al. 2016).

U. prolifera results in an extremely proliferative, albeit ephemeral community. It typically originates from aquaculture of the red macroalga *Porphyra yezoensis* along the Jiangsu coastline during mid-April to early May, then drifts northward and rapidly expands to bloom in the southern Yellow Sea for 1.5 months, and finally reaches the coast near Qingdao in July or August (Liu et al. 2010, Keesing et al. 2011, H. Li et al. 2016). In recent years, numerous surveys have been conducted to study the origin of the *U. prolifera* bloom (Pang et al. 2010, Zhang et al. 2011, Xiao et al. 2013), associated carbon fixation mechanisms (Xu et al. 2012), and growth and nutri-

*Corresponding author: roseliu@ouc.edu.cn

ent uptake of *U. prolifera* in the southern Yellow Sea (Teichberg et al. 2010, Shi et al. 2015, H. Li et al. 2016, 2017). Additionally, laboratory experiments showed that it could survive in a wide range of temperature, salinity, pH and irradiance conditions (Wang et al. 2007, Lin et al. 2011).

The outbreaks of algal blooms cause ecosystem changes in the region, especially changes in the chemical environment. For example, a significant drawdown in the partial pressure of CO_2 (pCO_2) in the Pearl River estuary was attributed to a phytoplankton bloom (Dai et al. 2008). An increase in dissolved inorganic carbon (DIC) and a decrease in pH, as well as abnormal total alkalinity (TA) values were reported in the southern Yellow Sea during the *U. prolifera* post-bloom period (Hu et al. 2015). To the best of our knowledge, there have been no reports about the carbonate system during the *U. prolifera* bloom period, and only 2 cruises were carried out by Hu et al. (2015) during the post-bloom period in 2008. In the present study, 2 cruises were conducted in coastal waters of Qingdao during the late bloom period and after the bloom in summer 2015. The aim was to better understand the influence of the *U. prolifera* bloom on the carbonate system and evaluate the effects of *U. prolifera* green tides on the ecological environment of a small region that was close to the coast but not subjected to the influence of terrestrial inputs. A parallel incubation experiment was also performed onboard the research vessel, to determine variations in the characteristics of the carbonate system in response to the decay of *U. prolifera*. This study thus aimed to improve our understanding of the biogeochemical response to this bloom event, with particular focus on the changes in the carbonate system in the context of ecosystem metabolism, and the response of the source or sink of CO_2 to the *U. prolifera* bloom during the late bloom period.

MATERIALS AND METHODS

Study area

Qingdao coastal waters, part of the southern Yellow Sea, are surrounded by the Shandong Peninsula and Jiaozhou Bay to the west (Fig. 1). Due to the shallow water depth and complex structure of the region, Qingdao coastal waters are dominated by semi-diurnal tidal currents (Zhao et al. 2011). Generally, *Ulva prolifera* initially appears in the Subei Shoal and then drifts to the southern Yellow Sea, where it grows rapidly into a green tide under favorable conditions. It is then transported to the Qingdao coast by surface ocean currents and the southeast monsoon in summer, and finally decays slowly and disappears in mid to late August (Hu et al. 2010, Keesing et al. 2011, Xu et al. 2016, Hu et al. 2017). The drift path and distribution of the bloom are provided by the North China Sea Branch of the State Oceanic Administration (SOA) (www.ncsb.gov.cn/n1/n127/n139/n39/index_5.html) (Fig. 2).

Two cruises were conducted on the RV 'Haidiao 235' during (1) the late bloom period, when thick accumulations of the green alga could still be observed at some stations, and (2) after the bloom period, when *U. prolifera* had disappeared from the coastal waters of Qingdao. The 2 cruises were carried

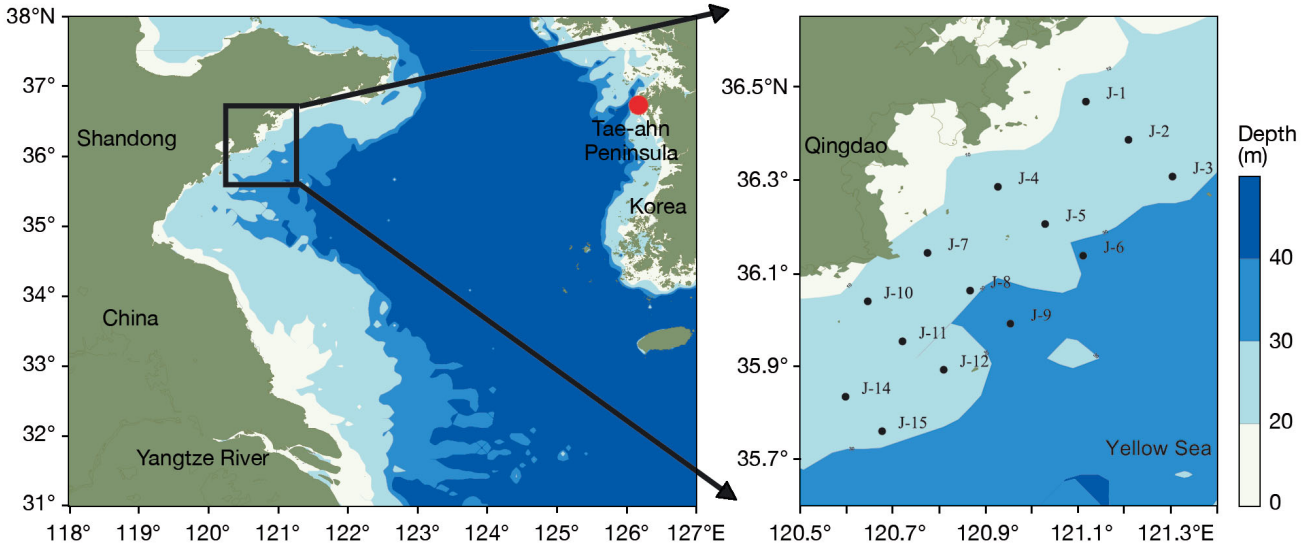

Fig. 1. Sampling stations (Stns J1–J15) in the coastal waters of Qingdao, southern Yellow Sea. Vertical color bar: water depth

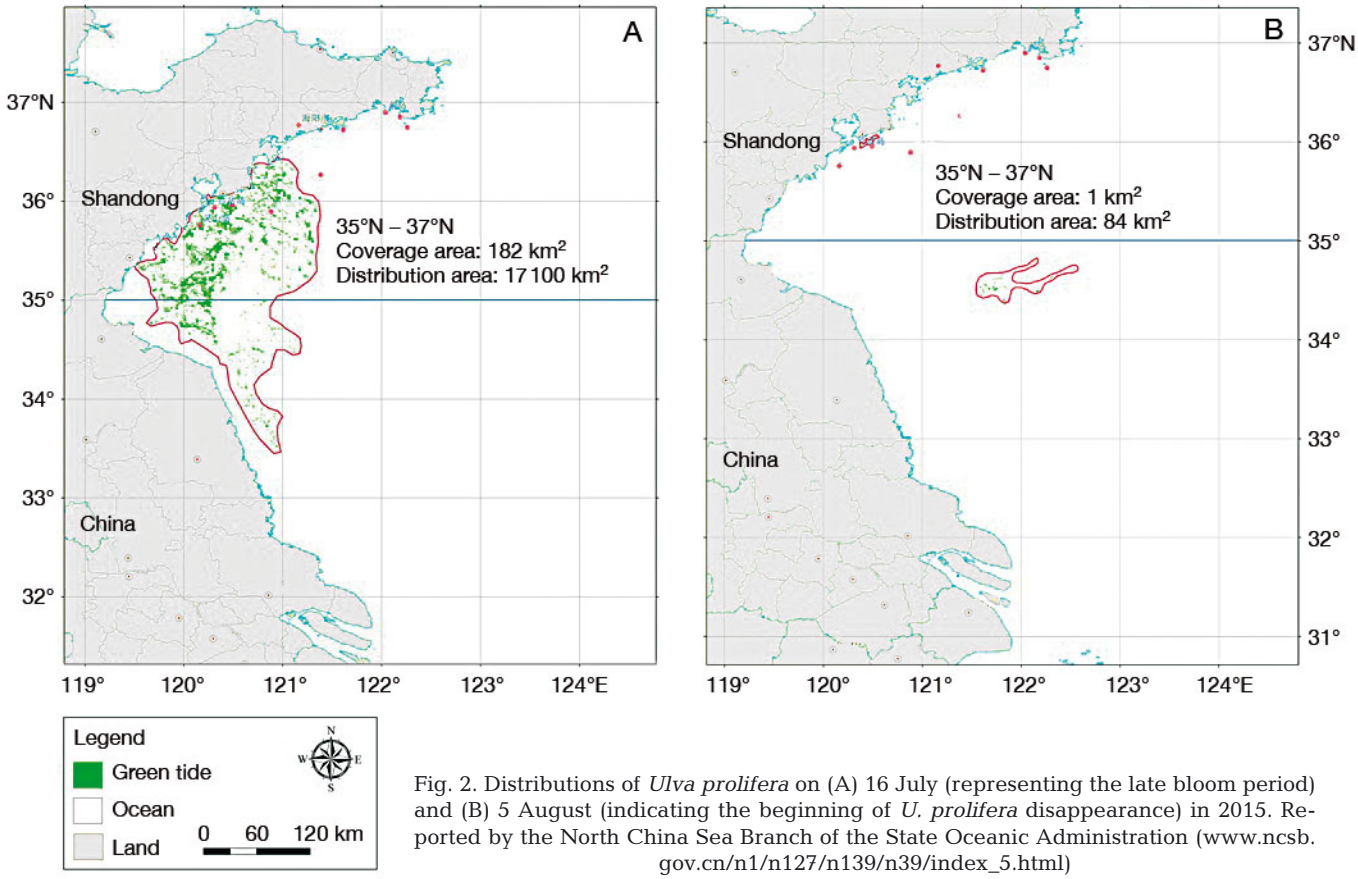

Fig. 2. Distributions of *Ulva prolifera* on (A) 16 July (representing the late bloom period) and (B) 5 August (indicating the beginning of *U. prolifera* disappearance) in 2015. Reported by the North China Sea Branch of the State Oceanic Administration (www.ncsb.gov.cn/n1/n127/n139/n39/index_5.html)

out on 16–17 July and 28–29 August 2015, respectively. The study area and observation stations are shown in Fig. 1. The distributions of *U. prolifera* on 16 July (representing the late bloom period) and 5 August (when the *U. prolifera* began to disappear) in 2015 are shown in Fig. 2. Thus, via these 2 cruises, the present study investigated the responses of the carbonate system to this *U. prolifera* bloom in the coastal waters of Qingdao.

Sampling

During the 2 cruises, temperature and salinity were recorded *in situ* with a conductivity, temperature, depth (CTD) sensor (Manta2; Eureka). When collecting samples for dissolved oxygen (DO), pH, DIC and TA, all bottles were allowed to overflow at least twice their volume to minimize contact with air. Samples for DO determination were collected using 125 ml glass bottles and immediately treated with the Winkler reagents (see below), and then sealed and immersed in ambient seawater. Discrete samples for DIC analysis were collected in 30 ml glass vials and TA samples (unfiltered and filtered; the TA values reported in this article refer to the former) were collected using 100 ml rigid polyethylene bottles; DIC and TA samples were preserved with 100 µl saturated $HgCl_2$ solution. An aliquot of 30 ml samples for dissolved organic carbon (DOC) was filtered through a 0.7 µm-pore Whatman glass fiber filter (GF/F) and stored frozen in glass bottles at –20°C. Chlorophyll *a* (chl *a*) samples were collected by filtering 300 ml of seawater through 0.7 µm-pore GF/F filters under low pressure (<15 kPa); filters were then frozen until analysis. In this study, the surface layer sampled corresponded to a depth of 0.5 m, the middle layer to a depth of 10 m and the bottom layer to a depth of 2 m from the bottom. All samples were taken onshore to the home laboratory and parameters were measured within several days of collection.

Incubation experiment

The effect of floating *U. prolifera* on the carbonate system of seawater was also examined via *in situ* incubation experiments in 5 l polyethylene bottles, filled with Qingdao coastal waters collected from 17 to 25 July 2015 and filtered onboard through a 0.2 µm

membrane filter (φ = 47 mm; Pall Corporation). The *U. prolifera* specimens were thoroughly washed and their epiphytes removed following macroalgal collection. According to the microscopic examination and identification by the Key Laboratory of Marine Genetics and Gene Resource Exploitation of the Ocean University of China, the growth of the algae was consistent with the standard characteristic of *U. prolifera*. Group 1 consisted of a blank with only filtered seawater, used as a control. Groups 2 and 3 were treated by adding 3 and 6 g wet weight of *U. prolifera* to 3 l of 0.2 µm-filtered seawater. All polyethylene bottles were maintained at *in situ* temperature by using a circulatory device whose water was provided continuously by shipboard ballast water. Cultivation of *U. prolifera* was established under the initial conditions of pH 8.03, DIC 2262 µmol kg^{-1}, TA 2342 µmol kg^{-1}, salinity 31.3, phosphate (PO_4^{3-}) 0.20 µmol l^{-1}, nitrate (NO_3^-) 3.16 µmol l^{-1}, nitrite (NO_2^-) 0.15 µmol l^{-1}, and ammonium (NH_4^+) 5.71 µmol l^{-1}. The ranges of temperature and light intensity were 15.46 to 25.92°C and 0.3 to 66 300.0 lx during the course of incubation, respectively. The bottles were gently shaken 3 times d^{-1} to ensure well-mixed nutrients. All treatments were conducted in duplicate and the incubation lasted for 8 d. The carbonate system parameters in the culture medium, including pH, DIC and TA, were measured every 2 d during the incubation period. In addition, statistical analyses were done using SPSS v.19.0, and results were considered significant at $p \leq 0.05$.

Analytical methods

The DIC concentrations of water samples were determined using a DIC analyzer (AS-C2; Apollo SciTech), with a precision of 0.1 to 0.2% (Cai & Wang 1998, Cai et al. 2004, Zhai et al. 2005). A 0.75 ml aliquot of the sample was pumped into the reactor and acidified by addition of 10% H_3PO_4, and the concentration of the extracted CO_2 gas was subsequently quantified with a Li-Cor CO_2 infrared detector (Wang & Cai 2004). The concentration of TA was determined using a 20 ml sample by Gran titration operated by a computer-controlled Kloehn digital pump; titration precision was 0.1% (Cai et al. 2004, Dai et al. 2008). Both the DIC and TA analyzers were calibrated using certified reference materials from A. G. Dickson's laboratory (Scripps Institution of Oceanography). For pH measurements, water samples were collected in narrow-mouth glass bottles and kept in a thermal bath (25 ± 0.1°C) for about 30 to 60 min. The pH was then measured onboard using a Ross Orion combination electrode (Ross-8102) and a Fisher pH meter (Star A211) on a National Bureau of Standards (NBS) scale (precision: ±0.005) and finally the values were corrected to the *in situ* temperature. The pCO_2 was calculated from the pH and DIC using CO_2SYS software (Pierrot et al. 2006) with the equilibrium constants determined based on Mehrbach (1973), refitted by Dickson & Millero (1987), and potassium bisulfate ($KHSO_4$) as described by Dickson (1990).

Air–water CO_2 fluxes (F, mmol m^{-2} d^{-1}) were estimated according to the following equation:

$$F = k \times \alpha \times \Delta pCO_2 \quad (1)$$

where k (cm h^{-1}) is the gas transfer velocity of CO_2, α is the solubility coefficient of CO_2 at the *in situ* temperature and salinity, and ΔpCO_2 is the difference between the water and air pCO_2. The atmospheric pCO_2 was acquired from the values measured at the Tae-ahn Peninsula (36.731° N, 126.131° E; red dot in Fig. 1), which was adjacent to the southern Yellow Sea. Positive flux values indicate the net CO_2 exchange from the water body to the atmosphere, while negative values represent the transfer of CO_2 from the atmosphere to the water. The calculations of k were based on the Wanninkhof (1992) empirical function of wind speed (since the *in situ k* value was not available), as follows:

$$k = 0.39 \times U \times (Sc / 660)^{-0.5} \quad (2)$$

where U (m s^{-1}) is the wind speed at 10 m height, here represented by long-term wind speed; Sc is the Schmidt number of CO_2 in seawater, and 660 is the the Sc value in seawater at 20°C.

The DOC concentration was determined by catalytic high temperature oxidation using a total organic carbon analyzer (Shimadzu TOC-V_{CPH}; Shimadzu) with platinum catalyst at 680°C. In order to eliminate the inorganic carbon component, the samples were acidified using 2 M HCl, and injected into the furnace by the autosampler; the combusted products (CO_2) were detected by the non-dispersive infrared gas analyzer. The precision was <2.0% (Yang et al. 2010).

Dissolved oxygen was measured using the Winkler method (Dickson 1995); $MnCl_2$ and alkaline KI solutions were added to DO bottles immediately after sampling with care taken not to introduce bubbles. Samples were maintained in the dark for at least 1 h before titration with the $Na_2S_2O_3$ solution under H_2SO_4 conditions. All samples were analyzed within 24 h of collection.

Chl *a* on the membrane was extracted with 90% acetone for 12 h in the dark at 4°C, centrifuged for 10 min, and then measured with a fluorescence

spectrophotometer (F-4500; Hitachi) according to Parsons et al. (1984). Because samples were filtered through Whatman GF/F membranes after the removal of *U. prolifera*, the concentrations of chl *a* in this study represent the biomass of micro-phytoplankton.

RESULTS

Temperature and salinity in coastal waters of Qingdao

The ranges and mean values of temperature and salinity are listed in Table 1. The vertical temperature profile decreased significantly with depth, while salinity showed a very slight increasing trend from the surface to the bottom layer. However, the water temperature and salinity did not show a detectable difference between the late bloom period and after the bloom. In the horizontal distribution, the temperature generally decreased from the coast to offshore waters, and salinity showed an opposite trend during both cruises (Figs. 3 & 4). Furthermore, the temperature and salinity were within suitable ranges for the growth of *Ulva prolifera* (temperature: 15 to 30°C, salinity: 16 to 40) during the 2 cruises (Gao et al. 2014).

Distributions of DO, chl *a* and DOC in coastal waters of Qingdao

The oxygen content of the water column indicated oversaturated conditions during both cruises. The highest DO value was obtained in the middle layer during the first cruise, while it exhibited a minimum value in the middle layer during the second cruise. It is notable that DO concentrations throughout the water column were lower in July than those in August, as shown in Table 1.

Concentrations of chl *a* were in the range of 0.01 to 0.21 µg l^{-1} in the surface seawater, with an average (±SD) value of 0.10 ± 0.06 µg l^{-1} during the first cruise. However, chl *a* concentrations increased to between 0.35 and 0.64 µg l^{-1} in the surface layer when *U. prolifera* was no longer present during the second cruise. Compared with the study period without *U. prolifera*, the average values of chl *a* were lower in all layers during the late bloom period (Table 1), which could be attributed to both the competition of *U. prolifera* with microalgae for nutrients and the inhibition of microalgal photosynthesis by the *U. prolifera* cover, and thus light attenuation in surface water.

Horizontal distributions of DOC are shown in Fig. 5. During the late bloom period, concentrations

Table 1. Ranges and means (in brackets) of hydrographic and carbonate system data during the *Ulva prolifera* late bloom and after the bloom in the coastal waters of Qingdao. DO: dissolved oxygen; DOC; dissolved organic carbon; DIC: dissolved inorganic carbon; TA: total alkalinity; pCO_2: partial pressure of CO_2

Parameter	Cruise	Surface layer	Middle layer	Bottom layer
Temperature (°C)	July	23.74–25.49 (24.39)	21.13–24.32 (22.86)	15.34–22.80 (19.93)
	August	22.67–26.38 (24.37)	18.85–24.53 (21.53)	15.34–21.54 (19.28)
Salinity	July	30.74–31.51 (31.14)	31.02–31.51 (31.26)	31.11–31.57 (31.34)
	August	30.82–31.57 (31.25)	30.98–31.46 (31.22)	31.02–31.38 (31.26)
DO (mg l^{-1})	July	6.44–6.88 (6.69)	6.26–7.13 (6.74)	5.33–7.13 (6.44)
	August	6.55–7.57 (7.16)	6.23–8.24 (7.08)	6.42–11.82 (8.97)
DOC (µmol kg^{-1})	July	61–183 (131)	61–240 (138)	80–190 (118)
	August	67–154 (130)	72–157 (127)	92–156 (129)
Chl *a* (µg l^{-1})	July	0.01–0.21 (0.10)	0.06–0.55 (0.25)	0.05–0.32 (0.18)
	August	0.35–0.64 (0.45)	0.23–0.35 (0.28)	0.23–0.42 (0.34)
DIC (µmol kg^{-1})	July	2008–2152 (2087)	2064–2174 (2097)	2048–2148 (2113)
	August	2032–2096 (2060)	2036–2194 (2071)	2074–2228 (2160)
TA (µmol kg^{-1})	July	2345–2414 (2385)	2348–2396 (2373)	2264–2455 (2388)
	August	2296–2349 (2328)	2297–2366 (2330)	2283–2356 (2333)
$TA_{(filtered)}$ (µmol kg^{-1})	July	2329–2392 (2365)	2319–2387 (2353)	2335–2356 (2317)
	August	2271–2335 (2311)	2271–2335 (2311)	2269–2343 (2319)
pH	July	7.99–8.11 (8.04)	7.90–8.06 (7.99)	7.84–8.02 (7.90)
	August	7.99–8.24 (8.10)	7.98–8.18 (8.09)	7.78–8.09 (7.88)
pCO_2 (µatm)	July	380.5–466.5 (427.0)	355.0–555.8 (450.2)	431.9–579.7 (506.6)
	August	245.5–471.8 (349.7)	224.1–441.9 (332.6)	316.5–680.5 (528.7)

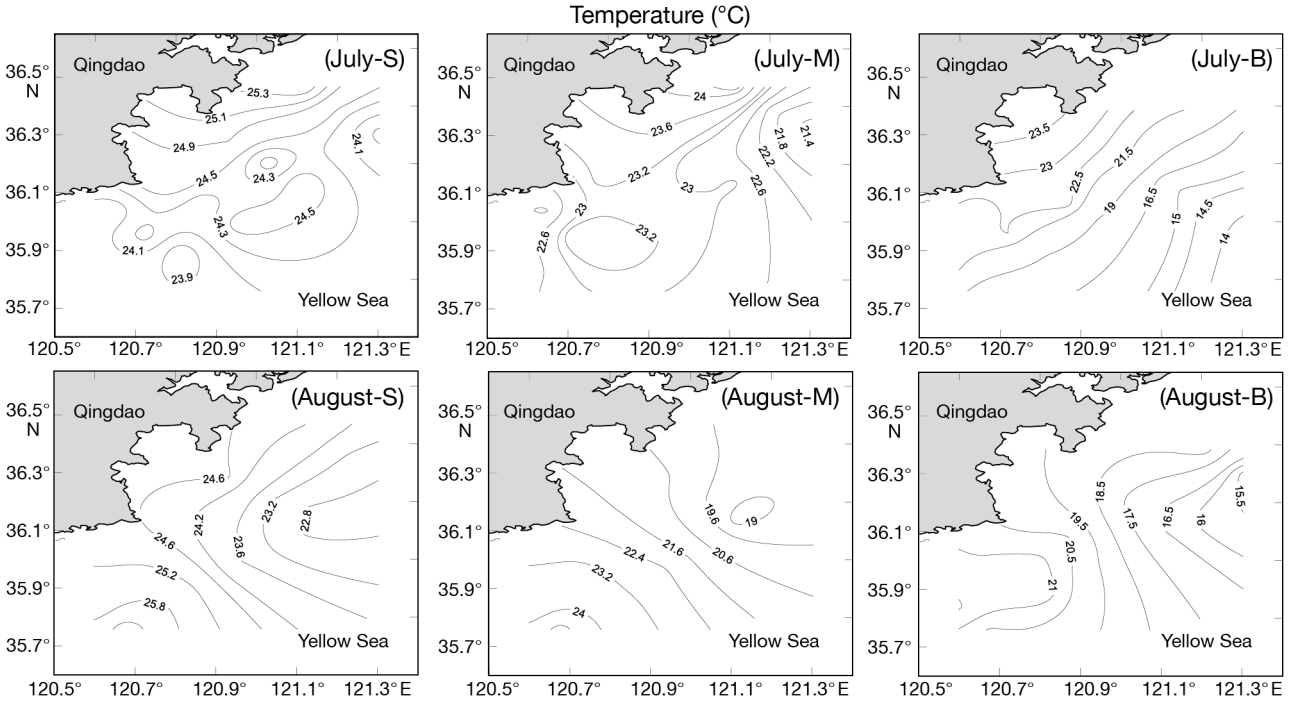

Fig. 3. Horizontal distributions of temperature (°C) in the surface (S), middle (M), and bottom (B) layers of the coastal waters of Qingdao during July and August

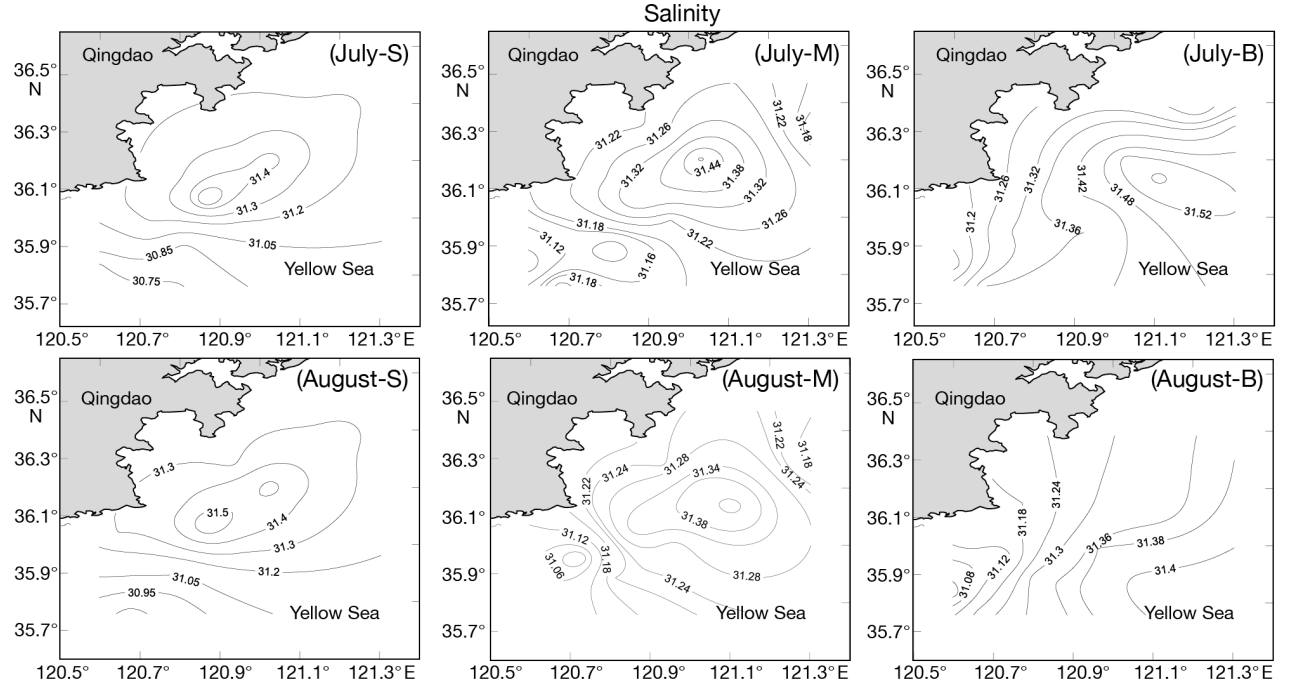

Fig. 4. Horizontal distributions of salinity in the surface (S), middle (M), and bottom (B) layers of the coastal waters of Qingdao during July and August

of DOC in surface waters generally decreased from inshore to offshore. The concentrations of DOC in the middle layer decreased at first and then increased from nearshore to offshore; the minimum value was obtained near Stn J5 (Fig. 1). Relatively high DOC concentrations were observed at inshore stations, and the concentration gradient was perpendicular to the shoreline in the bottom layer. After the bloom

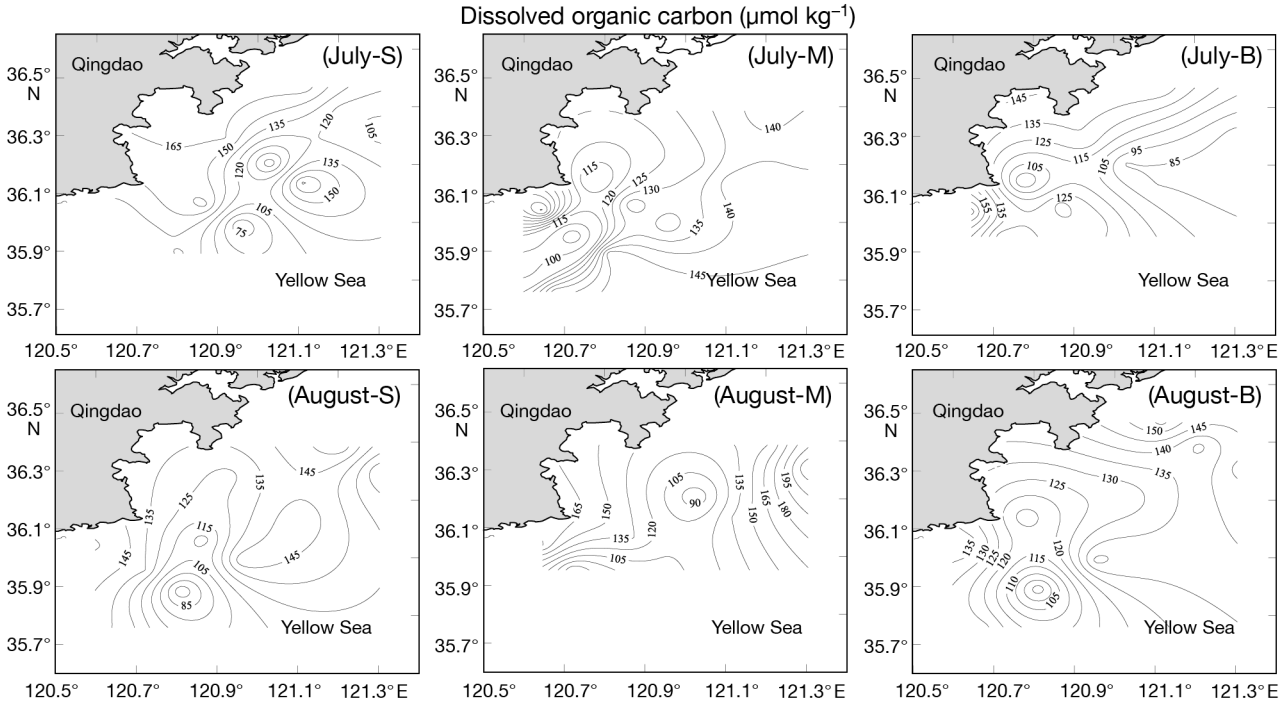

Fig. 5. Horizontal distributions of dissolved organic carbon (DOC; μmol kg^{-1}) in the surface (S), middle (M), and bottom (B) layers in the coastal waters of Qingdao during July and August

period, concentrations of DOC generally increased from south to north in the surface layer, and the location of the DOC minimum was in the vicinity of Stn J11 in the middle and bottom layers. Additionally, DOC concentrations in July were lower than those in August in the surface and bottom layers, while the concentrations of DOC in July were higher than those in August in the middle layer (Table 1).

Distributions of carbonate system parameters in coastal waters of Qingdao

The ranges and mean values of carbonate parameters (DIC, TA, pH and pCO_2) showed clear spatial and temporal differences. These are presented in Table 1 and Figs. 6–9.

Concentrations of DIC and pH in surface waters varied from 2008 to 2152 μmol kg^{-1}, and 7.99 to 8.11, respectively, with average values of 2087 ± 44 μmol kg^{-1} and 8.04 ± 0.03, respectively, during the first cruise. The vertical distribution of DIC increased gradually with depth, while pH exhibited an opposite trend throughout the water column. During the period of no detectable *U. prolifera*, DIC and pH in the surface layer were in the range of 2032 to 2096 μmol kg^{-1}, and 7.99 to 8.24, respectively, averaging 2060 ± 19 μmol kg^{-1} and 8.10 ± 0.08, respectively. The vertical variation in DIC and pH was generally similar to that observed during the late bloom period. In addition, TA values varied within a relatively narrow range, from 2345 to 2414 and 2296 to 2349 μmol kg^{-1}, respectively, during these 2 cruises.

During the first cruise, high DIC concentrations prevailed in the surface layer of inshore waters, and the concentration gradient was perpendicular to the shoreline. However, DIC showed an opposite trend in the bottom layer, and low DIC concentrations primarily occurred in Stn J6 and in the middle layer of the southwest portion of the study area (Fig. 6). As shown in Fig. 7, the horizontal distribution of TA in the surface layer showed an increasing trend from inshore to offshore waters, whereas TA concentrations in the middle layer showed only minor variation (2348 to 2396 μmol kg^{-1}) among the stations. The minimum value was obtained near Stn J10 in the bottom layer. During the second cruise, DIC showed distribution patterns similar to those observed during the first cruise (Fig. 6). The concentrations of TA increased from the coast to offshore waters in the surface and bottom layers, but not in the middle layer. The maximum concentration of TA was obtained near Stn J12 in the middle layer (Fig. 7).

The pH during the late bloom period increased in a northeast–southwest direction in surface water,

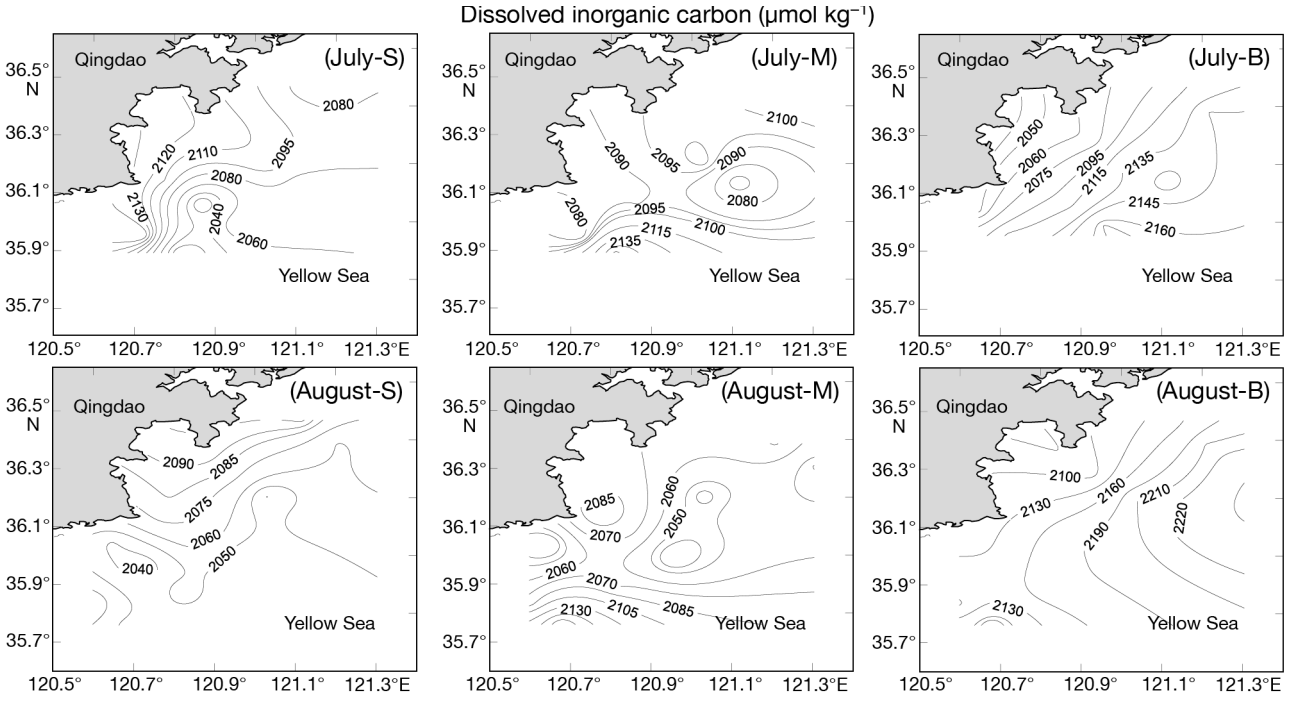

Fig. 6. Horizontal distributions of dissolved inorganic carbon (DIC; μmol kg^{-1}) in the surface (S), middle (M), and bottom (B) layers of the coastal waters of Qingdao during July and August

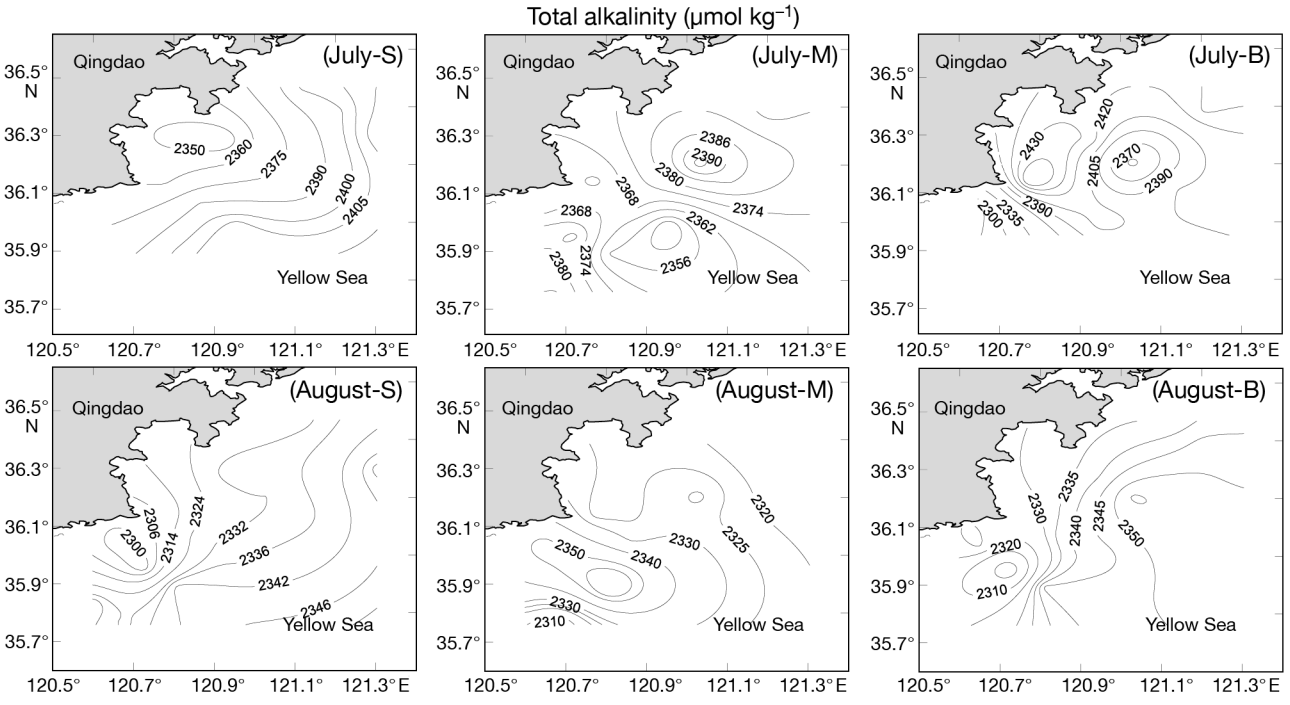

Fig. 7. Horizontal distributions of total alkalinity (TA; μmol kg^{-1}) in the surface (S), middle (M), and bottom (B) layers of the coastal waters of Qingdao during July and August

whereas it increased from nearshore to offshore waters in the middle layer of the study area, and exhibited a reverse trend in the bottom layer (Fig. 8). Conversely, pCO_2 increased in a stepwise manner from the south to the north in the surface layer of the study area, ranging from 381 to 466 μatm. It decreased from the coast to offshore waters, ranging between 355 and 556 μatm in the

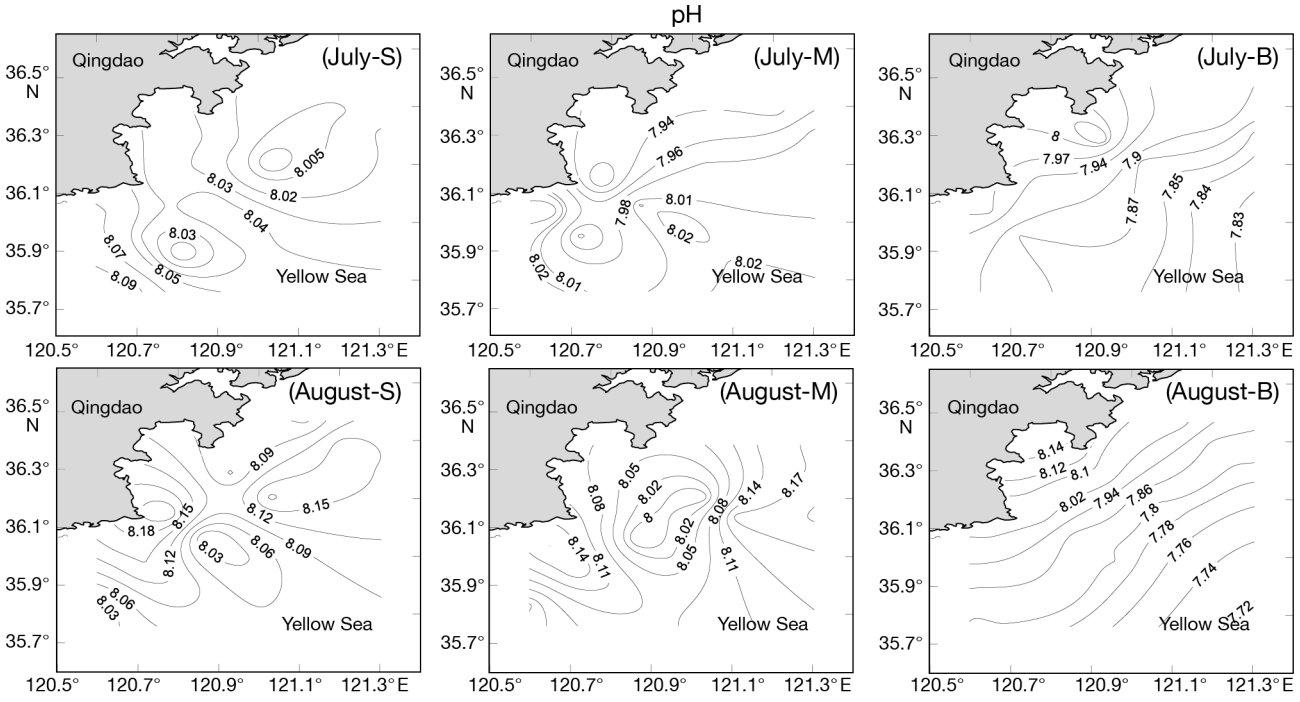

Fig. 8. Horizontal distributions of pH in the surface (S), middle (M), and bottom (B) layers of the coastal waters of Qingdao during July and August

middle layer. It initially increased and then decreased along an inshore to offshore direction in the bottom layer, and high pCO_2 values (580 and 591 µatm) were found at Stns J5 and J11, respectively (Fig. 9). Under conditions without *U. prolifera*, the pH in the surface layer generally decreased from inshore to offshore waters and relatively higher values (~8.20) were found along the coastline. A low pH value of 7.98 was recorded in the vicinity of Stn J8 in the middle layer, and the distribution pattern of pH in the bottom layer was generally consistent with that of the late bloom period. The pCO_2 in the surface layer increased from inshore to offshore waters and from the northern to the southern region with a range of 245 to 472 µatm. This parameter again increased from the north to the south in the middle layer, and gradually increased from inshore to offshore waters in the bottom layer. In general, the location of the pH minimum coincided with that of pCO_2 maximum.

Variations of the carbonate system parameters during the incubation experiment

Fig. 10 shows the incubation results from 17 to 25 July 2015. The carbonate system parameters of the incubation medium with *U. prolifera* were significantly higher than those of the control (1-way ANOVA, $p < 0.05$). There was no significant difference between incubations when 3 and 6 g wet weight of *U. prolifera* were added (1-way ANOVA, $p > 0.05$). To be specific, the pH of culture medium in Groups 2 and 3 increased gradually at first, attaining peak values of 8.35 ± 0.05 and 8.38 ± 0.02 on Day 4, and then decreased to 7.79 ± 0.08 and 7.81 ± 0.08 on Day 8, respectively. The pH values in Group 3 were slightly higher than those in Group 2 during the early stage of incubation, whereas the opposite trend was found during the later incubation period.

The DIC concentration in the culture medium of Groups 2 and 3 decreased by ca. 117 and 151 µmol kg^{-1}, respectively, within the first 2 d. Subsequently, the release of DIC from *U. prolifera* occurred rapidly, the concentration of DIC in the culture medium of Groups 2 and 3 increased by ca. 159 and 245 µmol kg^{-1}, respectively, from Day 2 to the end of the experiment. However, TA in the culture medium of Groups 2 and 3 increased to 2404 ± 4 and 2435 ± 7 µmol kg^{-1} initially, then decreased to 2326 ± 9 and 2342 ± 6 µmol kg^{-1}, and finally increased to 2366 ± 10 and 2392 ± 6 µmol kg^{-1}, respectively. The values of TA in Groups 2 and 3 on Day 8 were higher than their corresponding initial values. Variation patterns of DIC and TA in Group 2 were highly consistent with those in Group 3 (Fig. 10).

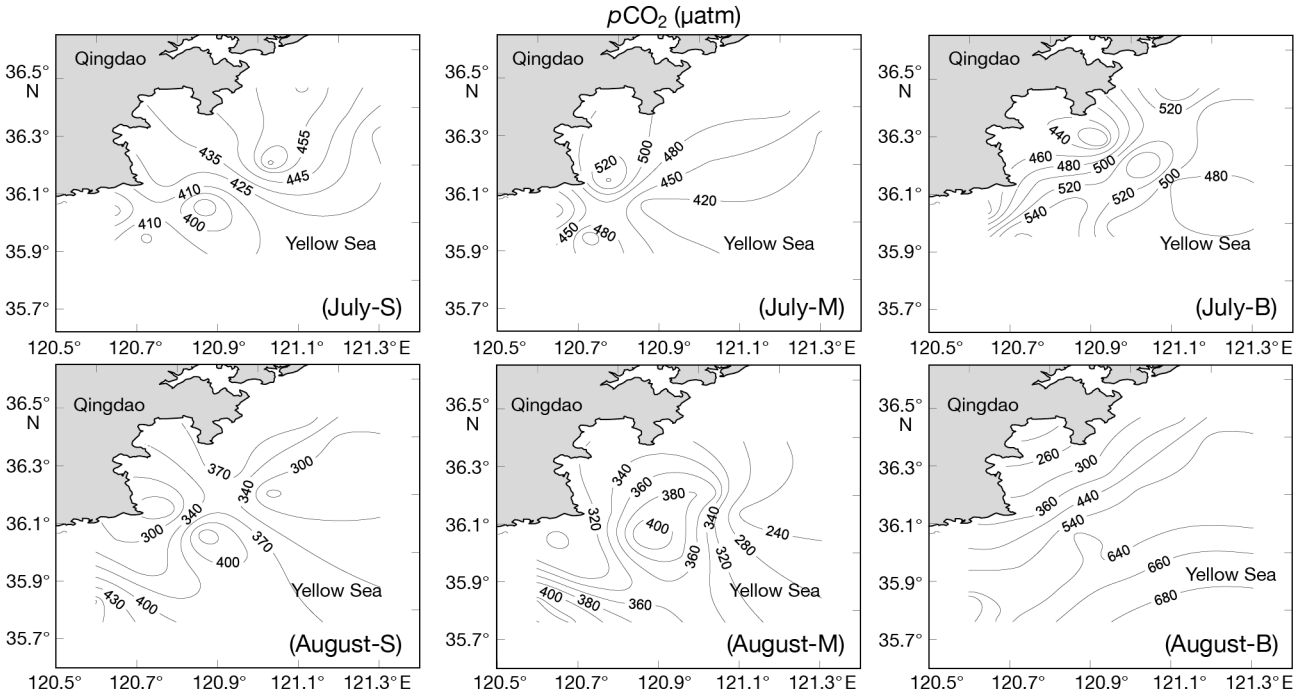

Fig. 9. Horizontal distributions of partial pressure of carbon dioxide (pCO_2; μatm) in the surface (S), middle (M), and bottom (B) layers of the coastal waters of Qingdao during July and August

DISCUSSION

Influence of the *Ulva prolifera* bloom on DO and pH

The content of DO in seawater is an important indicator of the biological growth and pollution status of a body of water. The main source of DO in seawater is the atmosphere, although DO can also be produced by planktonic and benthic algae via photosynthesis in the sea (Xia et al. 2009). As shown in Table 1, our entire study area was found to be rich in oxygen due to the fact that coastal waters were well-mixed by tidal currents (Qu et al. 2015). Nevertheless, the concentrations of oxygen throughout the water column in July were lower than those in August. This was most likely related to the fact that *Ulva prolifera* cover hindered the air–water exchange to some extent, which led to the limited decrease in DO in the late bloom regions (Gao et al. 2014).

As noted in Table 1, pH values in July were lower than those in August except for those in the bottom layer. This discrepancy could be attributed to floating of *U. prolifera* in the surface layer, which released a large amount of CO_2 via respiration and decomposition processes. Concurrently, the pH value on Day 8 of the incubation experiment was reduced by ~0.23 units compared with the initial value. This result was consistent with that of field observations obtained in the present study in the coastal waters of Qingdao, and it also agrees well with the estimate by Hu et al. (2015).

Response of the carbonate system to *U. prolifera* late bloom conditions

A plot of TA versus DIC was generated to account for the influence of water mixing. The TA–DIC relationship should be a straight line during simple water mixing (Dai et al. 2008). Fig. 11 portrays the variation of TA–DIC in the surface layer during the 2 cruises; however, there was no detectable correlation between the 2 parameters. According to the equation for biological oxygen consumption and respiration (Wang et al. 2003):

$$(CH_2O)_{106}(NH_3)_{16}H_3PO_4 + 138O_2 \rightarrow 106CO_2 + 16HNO_3 + H_3PO_4 + 122H_2O \quad (3)$$

every unit of Redfield-like organic matter produced or respired is associated with 106 units of DIC change, but only a small TA change (i.e. $\Delta DIC/\Delta TA = -106/17$) when significant photosynthesis or respiration occurs. Therefore, major departures from the straight line of mixing towards higher DIC values caused by biological release were observed during the late bloom period.

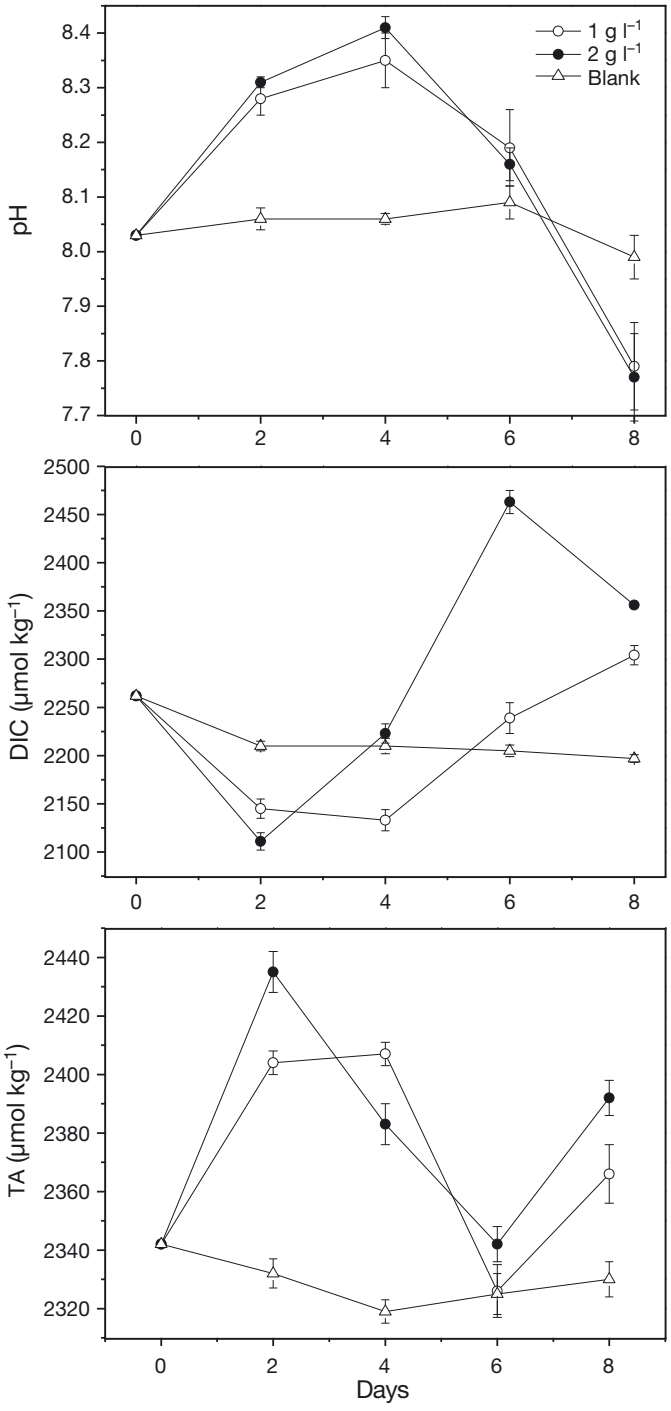

Fig. 10. Mean (±SD) variation in pH, dissolved inorganic carbon (DIC) and total alkalinity (TA) in the incubation experiments (n = 2)

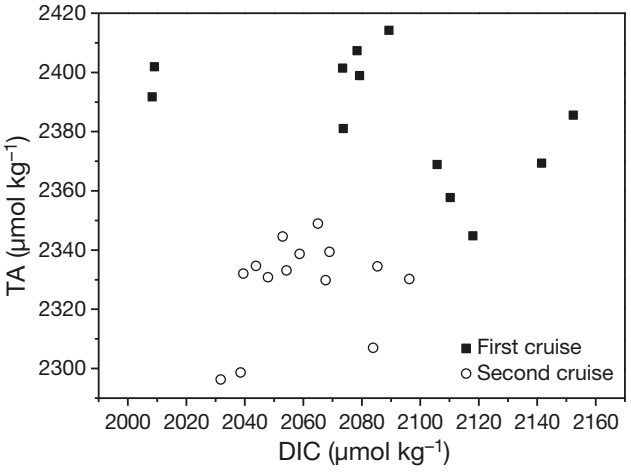

Fig. 11. Relationships between total alkalinity (TA) and dissolved inorganic carbon (DIC) in the surface layer of the coastal waters of Qingdao during the 2 cruises

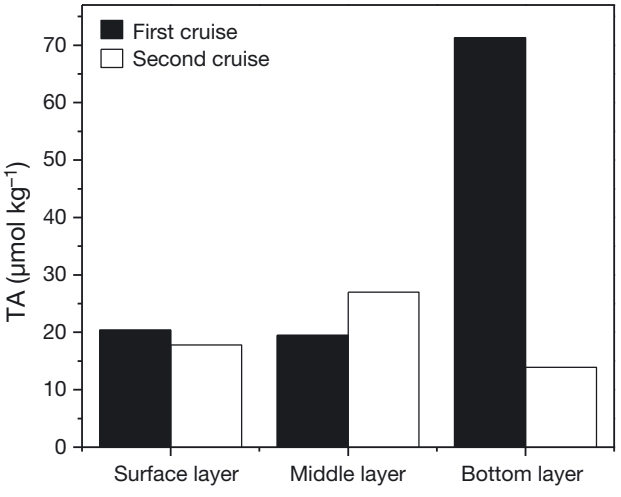

Fig. 12. Average difference in total alkalinity (ΔTA: $TA_{unfiltered}$ – $TA_{filtered}$) in different layers of the coastal waters of Qingdao during the 2 cruises

On the other hand, it is well known that most phytoplankton surfaces exhibit a net negative charge at neutral or high pH, because there are more abundant negatively charged carboxyl and phosphate groups than positively charged amino groups in seawater (Kleijn & Leeuwen 2000). The former reacts with protons during the titration of unfiltered seawater with hydrochloric acid, causing an increase in the measured alkalinity, especially during the late bloom period. In the present study, ΔTA ($TA_{unfiltered}$ – $TA_{filtered}$) was maintained within a narrow range, except for the abrupt increase to ca. 70 μmol kg^{-1} in bottom water during the first cruise (Fig. 12). This suggests that biogenic $CaCO_3$ and organic particles, suspended in deep waters, also contributed to the increase in the magnitude of ΔTA during the late bloom period (Kim et al. 2006).

Results from the incubation experiment provide clear evidence indicating that there was rapid

absorption of DIC by *U. prolifera* during the first 2 d, and rapid release of DIC during the next 6 d in the culture medium. For example, it can be estimated that the average absorption rates of DIC from *U. prolifera* at different densities were 59 µmol l^{-1} d^{-1} (at an algal density of 1 g l^{-1}) and 76 µmol l^{-1} d^{-1} (at an algal density of 2 g l^{-1}), during the first 2 d of the incubation experiment, while in the control group they decreased by 26 µmol l^{-1} d^{-1} during the first 2 d and subsequently remained relatively constant in the culture medium. In turn, the average release rates of DIC by *U. prolifera* were 27 µmol l^{-1} d^{-1} (at an algal density of 1 g l^{-1}) and 41 µmol l^{-1} d^{-1} (at an algal density of 2 g l^{-1}), respectively, during the next 6 d in the culture medium. This indicated that DIC absorption or the release rate by *U. prolifera* was positively correlated with the biomass of *U. prolifera* (over the relatively narrow biomass range tested) during the late bloom period. However, DIC absorption and release rates by *U. prolifera* were underestimated, since the atmosphere became a CO_2 source and atmospheric CO_2 entered the water body when DIC was absorbed by *U. prolifera*, while the atmosphere became a CO_2 sink and CO_2 in water entered atmosphere when DIC was released by *U. prolifera*. Moreover, the absorption of DIC by *U. prolifera* during the incubation experiment, when *U. prolifera* was decaying, was consistent with the results of the field study during the late bloom period.

Implications for changes of pCO_2 and air–water CO_2 fluxes during the *U. prolifera* late bloom

The average pCO_2 (±SD) in surface water was ca. 350 ± 75 µatm during the second survey, but it rose to a maximum of ca. 427 ±32 µatm in the surface layer during the late bloom period. According to the atmospheric CO_2 data (402 ppm in July 2015) from the flask measurements at the Tae-ahn Peninsula (36.731° N, 126.131° E) adjacent to the southern Yellow Sea, a sink of CO_2 in this region (Qu et al. 2015) was converted into a weak CO_2 source during the late bloom period. Concomitantly with the increase in pCO_2, a slight reduction in DO was also recorded, demonstrating that enhanced respiration by *U. prolifera* occurred during late bloom conditions. A lack of correlation between pCO_2 and temperature was observed during both cruises (Fig. 13). There was no statistically significant difference between pCO_2 and temperature during the first ($p = 0.086$) or second ($p = 0.226$) cruise, although temperature is the primary controlling factor for pCO_2 in seawater (Takahashi et al. 1993). In addition, the finding that water temperature did not show a detectable difference between the 2 cruises indicates that the significant difference in pCO_2 between the 2 cruises was not caused by temperature. In this study, biological activity (the process of decline of *U. prolifera*) was considered the main cause for this finding. It was attributed to the fact that the *U. prolifera* respiration exceeded photosynthesis and more CO_2 was released rather than absorbed during the late bloom period.

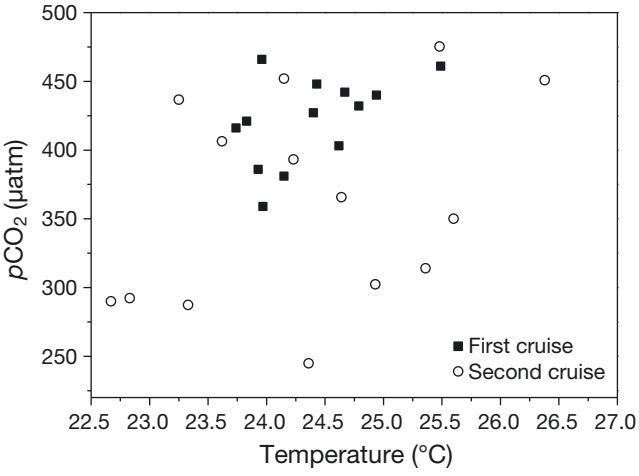

Fig. 13. Relationship between partial pressure of CO_2 (pCO_2) and temperature during the 2 cruises in the coastal waters of Qingdao

The average wind speeds (i.e. 3.73 and 3.65 m s^{-1}) in Qingdao coastal waters in July and August, respectively (Saha et al. 2014), were used to calculate the wind speed-dependent CO_2 gas transfer coefficient of Wanninkhof (1992). The estimated air–water CO_2 fluxes of the coastal waters off Qingdao ranged from −0.72 to 2.17 mmol m^{-2} d^{-1} and from −5.06 to 2.36 mmol m^{-2} d^{-1}, with mean values of 0.82 ± 0.88 and −1.31 ± 2.41 mmol m^{-2} d^{-1} during the late bloom and after bloom periods, respectively. In general, the pCO_2 in seawater exceeded the pCO_2 in the atmosphere, which led to outgassing of CO_2 from seawater under the late bloom conditions. Based on reports that the areal cover of the green tide in coastal waters off Qingdao attained up to 182 km^2 on 16 July 2015 (North China Sea Branch of the SOA 2015) (Fig. 2), the carbon fluxes from the coastal waters off Qingdao to the atmosphere were calculated at ~1.79 t C d^{-1} during the late bloom period. Thus, the rapid release of CO_2 from the relatively short, late bloom *U. prolifera* period could have a significant effect on the ecosystem in coastal waters and directly affected the biogeochemical cycle of carbon in seawater.

CONCLUSIONS

Compared with the conditions recorded after the bloom, DIC, TA and pCO_2 were increased while pH was decreased during the *Ulva prolifera* late bloom period. Likewise, the observed variations in the carbonate system during the incubation experiment matched well with results obtained during the field surveys. The sink of atmospheric CO_2 in coastal waters off Qingdao was converted to a weak source of CO_2 as the *U. prolifera* decayed during the late bloom period. Furthermore, quantitative assessment of CO_2 fluxes during such intense bloom events, especially in coastal waters, should be taken into consideration in the assessment of air–water CO_2 fluxes. To enhance the understanding of the effects of such *U. prolifera* blooms on the carbonate system, continuous *in situ* monitoring on a larger spatial and temporal scale should be conducted in the future.

Acknowledgements. The authors thank the captain and crews of the RV 'Haidiao 235' for their help during the in situ investigation. This work was financially supported by the National Natural Science Foundation of China (Grant No. 41676065), the Fundamental Research Funds for the Central Universities (No. 201762032), and the National Key Research and Development Program of China (Grants No. 2016YFA0601301 and 2016YFC1402101).

LITERATURE CITED

Cai WJ, Wang Y (1998) The chemistry, fluxes, and sources of carbon dioxide in the estuarine waters of the Satilla and Altamaha Rivers, Georgia. Limnol Oceanogr 43: 657–668

Cai WJ, Dai M, Wang Y, Zhai W and others (2004) The biogeochemistry of inorganic carbon and nutrients in the Pearl River estuary and the adjacent Northern South China Sea. Cont Shelf Res 24:1301–1319

Dai M, Zhai W, Cai WJ, Callahan J and others (2008) Effects of an estuarine plume-associated bloom on the carbonate system in the lower reaches of the Pearl River estuary and the coastal zone of the northern South China Sea. Cont Shelf Res 28:1416–1423

Dickson AG (1990) Standard potential of the reaction: $AgCl(s) + 12H_2(g) = Ag(s) + HCl(aq)$, and the standard acidity constant of the ion HSO_4^- in synthetic sea water from 273.15 to 318.15 K. J Chem Thermodyn 22:113–127

Dickson AG (1995) Determination of dissolved oxygen in seawater by Winkler titration. World Ocean Circulation Experiment (WOCE) operations manual, part 3.13: WHP operations and methods. WHP Office Report WHPO 91-1, Woods Hole, MA

Dickson AG, Millero FJ (1987) A comparison of the equilibrium constants for the dissociation of carbonic acid in seawater media. Deep-Sea Res A, Oceanogr Res Pap 34: 1733–1743

Gao S, Fan SL, Han XR, Yan LI, Wang T, Shi XY (2014) Relations of *Enteromorpha prolifera* blooms with temperature, salinity, dissolved oxygen and pH in the southern Yellow Sea. China Environ Sci 34:213–218

Guidone M, Thornber CS (2013) Examination of *Ulva* bloom species richness and relative abundance reveals two cryptically co-occurring bloom species in Narragansett Bay, Rhode Island. Harmful Algae 24:1–9

Hu C, Li D, Chen C, Ge J and others (2010) On the recurrent *Ulva prolifera* blooms in the Yellow Sea and East China Sea. J Geophys Res 115:C05017

Hu YB, Liu CY, Yang GP, Zhang HH (2015) The response of the carbonate system to a green algal bloom during the post-bloom period in the southern Yellow Sea. Cont Shelf Res 94:1–7

Hu LB, Hu CM, He MX (2017) Remote estimation of biomass of *Ulva prolifera* macroalgae in the Yellow Sea. Remote Sens Environ 192:217–227

Keesing JK, Liu D, Fearns P, Garcia R (2011) Inter- and intra-annual patterns of *Ulva prolifera* green tides in the Yellow Sea during 2007-2009, their origin and relationship to the expansion of coastal seaweed aquaculture in China. Mar Pollut Bull 62:1169–1182

Kim HC, Lee K, Choi W (2006) Contribution of phytoplankton and bacterial cells to the measured alkalinity of seawater. Limnol Oceanogr 51:331–338

Kleijn JM, Leeuwen HP (2000) Electrostatic and electrodynamic properties of biological interphases. In: Baszkin A, Norde W (eds) Physical chemistry of biological interfaces. Marcel Dekker, New York, NY, p 49–83

Li H, Zhang Y, Han X, Shi X, Rivkin RB, Louis L (2016) Growth responses of *Ulva prolifera* to inorganic and organic nutrients: implications for macroalgal blooms in the southern Yellow Sea, China. Sci Rep 6:26498

Li H, Zhang Y, Tang H, Shi X, Rivkin RB, Legendre L (2017) Spatiotemporal variations of inorganic nutrients along the Jiangsu coast, China, and the occurrence of macroalgal blooms (green tides) in the southern Yellow Sea. Harmful Algae 63:164–172

Li Y, Huang HJ, Li H, Liu J, Yang W (2016) Genetic diversity of *Ulva prolifera* population in Qingdao coastal water during the green algal blooms revealed by microsatellite. Mar Pollut Bull 111:237–246

Lin AP, Wang C, Pan GH, Song LY and others (2011) Diluted seawater promoted the green tide of *Ulva prolifera* (Chlorophyta, Ulvales). Phycol Res 59:295–304

Liu D, Keesing JK, Dong Z, Zhen Y and others (2010) Recurrence of the world's largest green-tide in 2009 in Yellow Sea, China: *Porphyra yezoensis* aquaculture rafts confirmed as nursery for macroalgal blooms. Mar Pollut Bull 60:1423–1432

Mehrbach C (1973) Measurement of the apparent dissociation constants of carbonic acid in seawater at atmospheric pressure. Limnol Oceanogr 18:897–907

North China Sea Branch of the SOA (State Ocean Administration) (2015) The drift path and distribution of the bloom. www.ncsb.gov.cn/n1/n127/n39/index.html (in Chinese)

Pang SJ, Feng L, Shan TF, Xu N and others (2010) Tracking the algal origin of the *Ulva* bloom in the Yellow Sea by a combination of molecular, morphological and physiological analyses. Mar Environ Res 69:207–215

Parsons TR, Maita Y, Lalli CM (1984) A manual of chemical and biological methods for seawater analysis. Pergamon Press, Oxford

Pierrot D, Lewis E, Wallace R, Wallace D, Wallace W, Wallace DWR (2006) MS Excel program developed for CO_2

system calculations. ORNL/CDIAC-105a. Carbon Dioxide Information Analysis Center, Oak Ridge National Laboratory, US Department of Energy, Oak Ridge, TN

Qu B, Song J, Yuan H, Li X and others (2015) Summer carbonate chemistry dynamics in the southern Yellow Sea and the East China Sea: regional variations and controls. Cont Shelf Res 111:250–261

Saha S, Moorthi S, Wu X, Wang J and others (2014) The NCEP climate forecast system version 2. J Clim 27: 2185–2208

Shi X, Qi M, Tang H, Han X (2015) Spatial and temporal nutrient variations in the Yellow Sea and their effects on *Ulva prolifera* blooms. Estuar Coast Shelf Sci 163:36–43

Takahashi T, Olafsson J, Goddard JG, Chipman DW, Sutherland SC (1993) Seasonal variation of CO_2 and nutrients in the high-latitude surface oceans: a comparative study. Global Biogeochem Cycles 7:843–848

Teichberg M, Fox SE, Olsen YS, Valiela I and others (2010) Eutrophication and macroalgal blooms in temperate and tropical coastal waters: nutrient enrichment experiments with *Ulva* spp. Glob Change Biol 16:2624–2637

Wang B, Chen A, Liu F (2003) Study on Redfield ratios in the world ocean. Adv Mar Sci 21:232–235

Wang J, Yan B, Lin A, Jinping HU, Shen S (2007) Ecological factor research on the growth and induction of spores release in *Enteromorpha prolifera* (Chlorophyta). Mar Sci Bull 26:60–65

Wang ZA, Cai WJ (2004) Carbon dioxide degassing and inorganic carbon export from a marsh dominated estuary (the Duplin River): a marsh CO_2 pump. Limnol Oceanogr 49:341–354

Wanninkhof R (1992) Relationship between wind speed and gas exchange over the ocean. J Geophys Res Atmos 97: 7373–7382

Xia B, Ma SS, Cui Y, Chen BJ and others (2009) Distribution of temperature, salinity, dissolved oxygen, nutrients and their relationships with green tide in *Enteromorpha prolifera* outbreak area of the Yellow Sea. Prog Fish Sci 30:94–101

Xiao J, Li Y, Song W, Wang Z and others (2013) Discrimination of the common macroalgae (*Ulva* and *Blidingia*) in coastal waters of Yellow Sea, northern China, based on restriction fragment-length polymorphism (RFLP) analysis. Harmful Algae 27:130–137

Xu J, Xiao F, Zhang X, Dong X and others (2012) Evidence of coexistence of C_3 and C_4 photosynthetic pathways in a green-tide-forming alga, *Ulva prolifera*. PLOS ONE 7: e37438

Xu Q, Zhang H, Cheng Y, Zhang S, Zhang W (2016) Monitoring and tracking the green tide in the Yellow Sea with satellite imagery and trajectory model. IEEE J Sel Top Appl Earth Obs Remote Sens 9:5172–5181

Yang GP, Zhang YP, Lu XL, Ding HB (2010) Distributions and seasonal variations of dissolved carbohydrates in the Jiaozhou Bay, China. Estuar Coast Shelf Sci 88:12–20

Ye NH, Zhang XW, Mao YZ, Liang CW and others (2011) 'Green tides' are overwhelming the coastline of our blue planet: taking the world's largest example. Ecol Res 26: 477–485

Zhai WD, Dai MH, Cai WJ, Wang YC, Wang ZH (2005) High partial pressure of CO_2 and its maintaining mechanism in a subtropical estuary: the Pearl River estuary, China. Mar Chem 93:21–32

Zhang X, Dong X, Mao Y, Li Y and others (2011) Settlement of vegetative fragments of *Ulva prolifera* confirmed as an important seed source for succession of a large-scale green tide bloom. Limnol Oceanogr 56:233–242

Zhao J, Chen X, Hu W, Chen J, Guo M (2011) Dynamics of surface currents over Qingdao coastal waters in August 2008. J Geophy Res 116:C10020

Editorial responsibility: Just Cebrian, Dauphin Island, Alabama, USA

Submitted: October 3, 2017; Accepted: August 28, 2018
Proofs received from author(s): October 18, 2018